Journal of Alloys and Compounds 884 (2021) 160927

Contents lists available at ScienceDirect

Journal of Alloys and Compounds

journal homepage: www.elsevier.com/locate/jalcom

One-step combustion synthesis of carbon-coated NiO/Ni composites for lithium and sodium storage

Chunxiao Xu[a,b], Yayong Li[a], Ryan A. Adams[c], Vilas G. Pol[c], Yang Xiao[c,*], Arvind Varma[c,1], Pengwan Chen[a,*]

[a] State Key Laboratory of Explosion Science and Technology, Beijing Institute of Technology, 5 South Zhongguancun Street, Haidian District, Beijing 100081, PR China
[b] Aerospace Institute of Advanced Materials & Processing Technology, No. 40 Yard Yungang North Residential Community, Fengtai, Beijing 100074, PR China
[c] Davidson School of Chemical Engineering, Purdue University, 480 Stadium Mall Drive, West Lafayette, IN 47907, United States

ARTICLE INFO

Article history:
Received 24 March 2021
Received in revised form 2 June 2021
Accepted 20 June 2021
Available online 27 June 2021

Keywords:
Combustion synthesis
CO_2 reduction
Carbon coating
Nickel oxide
Lithium ion battery
Sodium ion battery

ABSTRACT

Using carbon dioxide and nickel nitrate as the carbon and nickel sources respectively, a carbon-coated NiO/Ni (NiO/Ni@C) composite was synthesized *via* a one-step solution combustion method. Ethanolamine was used as the CO_2 adsorption solution, with nickel nitrate dissolved in it to form the combustion precursor at a molecular level. The as-obtained NiO/Ni nanoparticles exhibited spherical morphology with an average size of 30 nm, and controlled carbon content ranging from 50 to 90 wt%. The NiO/Ni@C composites were investigated as anode material for lithium and sodium ion batteries, exhibiting high reversible specific capacity and excellent rate performance. The NiO/Ni@C-0.25 sample showed a reversible capacity of 125 mAh g^{-1} with a specific current of 0.1 A g^{-1} as sodium ion anode, and a capacity of 791 mAh g^{-1} with a specific current of 0.1 A g^{-1} after 150 cycles as lithium ion anode. Owing to the novel one-step combustion process and resulting superior electrochemical performance, the NiO/Ni@C composite is demonstrated as a prospective anode material for rechargeable lithium and sodium ion batteries.

1. Introduction

Owing to the features of high specific energy, low self-discharge rate, moderate cycle life, and no memory effect, lithium-ion batteries (LIBs) are considered the premier high-efficiency secondary battery and the fastest-developing energy storage system. Anode material is one of the important factors affecting the electrochemical performance of LIBs. Currently, graphite, the commercial anode material, is limited by its low theoretical specific capacity, which limits the development of electric vehicles [1]. Therefore, the search for new anode materials has been a popular research area. Nano-sized transition metal oxides such as Fe_3O_4, NiO, CuO, $ZnCo_2O_4$, $Li_4Ti_5O_{12}$ have been reported to show promising electrochemical properties as anode materials for LIBs [2–6]. Among them, NiO is an ideal anode material due to its high theoretical lithium storage capacity of 718 mAh g^{-1}, low cost, nontoxicity, and large reserves.

Unfortunately, due to poor conductivity and large volumetric changes upon lithiation, the resulting pulverization of NiO anode causes a rapid decay in the battery capacity and cycling stability [7]. Recent studies have shown that specially designed NiO nanostructures can alleviate these issues, such as nanoparticles, nanotubes, composite structures, etc [8,9]. by increasing the specific surface area of NiO and shorting the lithium ion diffusion path. Liu et al. used the template method to prepare NiO hollow nanotubes, which delivered a capacity of 600 mAh g^{-1} after 100 cycles at 200 mA g^{-1} [10]. Evmenenko et al. demonstrated that nanometer-scale Ni layers help initiate the conversion process at the electrolyte interface, while providing an architecture that confines the lithiation into the individual oxide. The Ni/NiO multilayer electrode exhibited a reversible capacity of 800 mAh g^{-1} after 100 cycles [11]. Another strategy is to combine NiO with carbon materials such as carbon nanotubes, graphite, nanofibers, porous carbon, etc [12–14]. Increasing the conductivity of NiO alleviates the pulverization due to volumetric changes of NiO to a certain extent, which is beneficial in improving the cycling stability of the battery. Zhao et al. prepared a unique two-dimensional graphene/NiO composite material by self-assembling Ni directly on the surface of graphene oxide, resulting in

* Corresponding authors.
E-mail addresses: xiao63@purdue.edu (Y. Xiao), pwchen@bit.edu.cn (P. Chen).
[1] Deceased author

https://doi.org/10.1016/j.jallcom.2021.160927
0925-8388/

a high surface area of 134.5 m^2 g^{-1} and promising electrochemical performance [15]. Zou et al. obtained hierarchical hollow NiO/Ni/graphene composites, which exhibit a high reversible specific capacity of 1144 mAh g^{-1} after 1000 cycles as a lithium ion anode [16]. It is worth noting that carbon-coated metal/metal oxide composites possess multiple material property advantages, such as high electrical conductivity and fast charge transfer reaction kinetics, leading to augmented electrochemical performance.

To achieve the synergistic effect produced by the above characteristics, a carbon-coated NiO/Ni composite (NiO/Ni@C) was synthesized by a one-step solution combustion method. Carbon dioxide was used as the carbon source, and ethanolamine (MEA) was used as the solution for both CO_2 adsorption and the combustion reaction. In our earlier study, gaseous CO_2 was adsorbed into a hydrazine monohydrate solution to generate functional carbon foam through the solution combustion process, confirming that carbon can be produced directly from CO_2 by this methodology [17]. Compared to hydrazine hydrate, MEA offers decreased toxicity and corrosivity, and thus has been used in industry for chemical sorption of CO_2. In this work, we introduce MEA as the CO_2 adsorption solution, with nickel nitrate dissolving in it to form the combustion precursor at the molecular level. As far as we know, this is a first report demonstrating the conversion of CO_2 into porous carbon-coated metal oxide composites through a solution combustion process. Notably, the carbon content can be easily controlled, ranging from 50 to 90 wt %., by varying the amount of nickel nitrate during the combustion process. The as-prepared NiO/Ni@C composites possess a high specific surface area of 245 m^2 g^{-1} and a pore volume of 0.769 cm^3 g^{-1}. As anode material for LIBs, the NiO/Ni@C composites exhibited excellent rate performance and NiO/Ni@C-0.25 sample showed a reversible capacity of 791 mAh g^{-1} at 0.1 A g^{-1} after 150 cycles. Additionally, this novel anode was used in a sodium-ion battery (SIB), which is an attractive energy storage system owing to the features of low-cost and sustainable for grid storage [18,19]. The initial investigation showed a reversible capacity of 125 mAh g^{-1} with a specific current of 0.1 A g^{-1}, suggesting the NiO/Ni@C composite as a prospective anode material for rechargeable SIBs.

2. Experimental

2.1. Synthesis of NiO/Ni@C composites

Scheme 1 illustrates the process to prepare NiO/Ni@C composites including adsorption of carbon dioxide gas into MEA solution, the addition of nickel nitrate and magnesium powder as reaction precursors, and synthesis of carbon-coated NiO/Ni composites by the combustion process. First, carbon dioxide gas was adsorbed by the alkaline MEA solution at room temperature, generating a carbamate solution. Then, nickel nitrate and magnesium powder were added in this order. Magnesium powder reacted with the above carbamate solution to form a stable complex sol. Specifically, magnesium powder spontaneously reacted with the ammonium cation in the carbamate solution, generating hydrogen and magnesium ions. Subsequently, the magnesium ions continued to complex with carbamic acid in the carbamate solution to form a complex sol, enabling nickel nitrate to dissolve in it. Self-propagating combustion [20] was initiated by tungsten wire ignition in air atmosphere, for one-step synthesis of a carbon-coated NiO/Ni composite nanomaterial. Through the above process, the physicochemical properties of the product could be controlled by varying the combustion precursor and environment, including the ratios of precursors in the MEA solution, and the different adsorption solutions as well as metal nitrate precursors.

The specific experimental procedure was as follows. Carbon dioxide was introduced into the MEA solvent to form a carbamate solution. The carbon dioxide saturated adsorption capacity was 70 mol%. Next, 7.64 g of the adsorption-stable carbamate solution was added to a quartz crucible, nickel nitrate was added according to the molar ratio of the intermediate product carbamate to nickel nitrate hexahydrate (1:0.05, 1: 0.125, 1: 0.25, 1:0.375), and finally an excess of magnesium powder (2.55 g) was added. The above mixture was placed on an electric oven (90 °C) and heated for 10 min to form a complex sol precursor uniformly mixed at the molecular level. The reactants were ignited by heating with a tungsten wire and subjected to a self-propagating combustion process in air for about 20 s. The changing curve of combustion temperature with time was detected in real-time using a 0.2 mm diameter K-type thermocouple (Omega). Then, the gray-color product was etched with 1 M HCl for 30 min to remove MgO impurities. After filtration, carbon-coated NiO/Ni nanomaterials were collected, washed repeatedly with deionized water, and subsequently vacuum freeze-dried to obtain the final product, which was labeled as NiO/Ni@C-0.05, −0.125, −0.25, −0.375, respectively.

2.2. Physicochemical characterization

The morphology of the samples was characterized by a Hitachi S-4800 scanning electron microscope (SEM) and a JEM-2010 transmission electron microscope (TEM). X 'pert pro MPD diffractometer (X-ray source is CuKα wavelength is 0.154 nm) was used to test the X-ray diffraction (XRD). Nitrogen adsorption and desorption experiments were carried out with a Quantachrome Autosorb-IQ-MP device at 77 K. Before nitrogen adsorption, the sample was degassed under vacuum at 243 K temperature for 10 h. Specific surface area

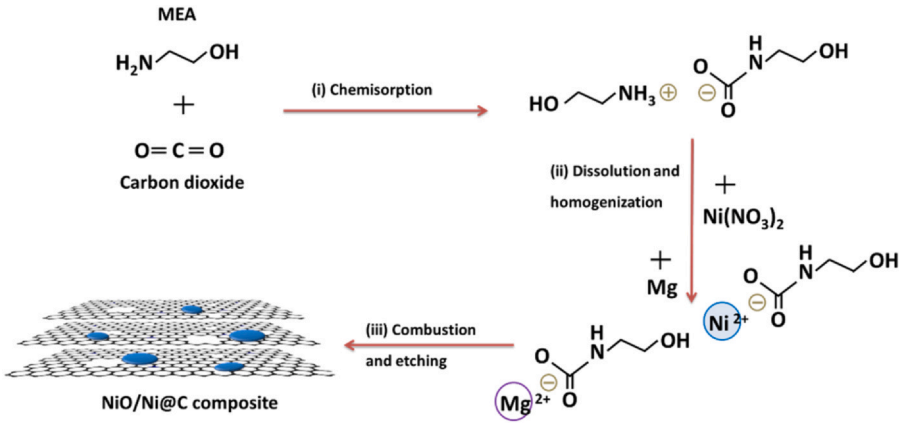

Scheme 1. The chemical process for combustion synthesis of NiO/Ni@C composites. (i) Adsorption of carbon dioxide gas into MEA solution. (ii) Addition of nickel nitrate and magnesium powder as reaction precursors. (iii) Combustion synthesis of carbon-coated NiO/Ni composites and dissolution of Mg and MgO during etching process.

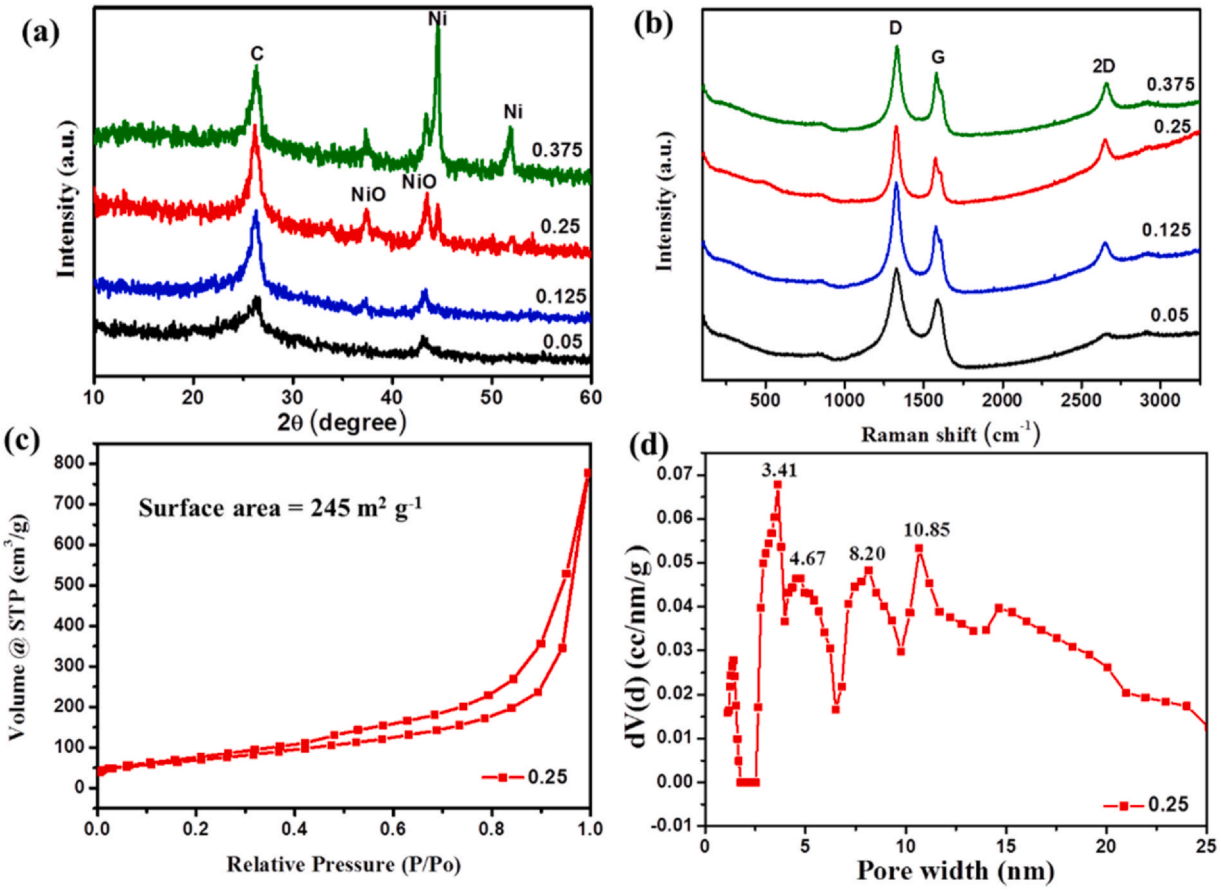

Fig. 1. Material characterization of NiO/Ni@C composites. (a) XRD and (b) Raman spectra. (c) Nitrogen adsorption-desorption curve of NiO/Ni@C-0.25 sample and (d) pore diameter distribution curve calculated by the corresponding DFT method.

(SSA) and pore diameter distribution were obtained by the Brunauer-Emmett-Teller (BET) and Density Functional Theory (DFT) methods. Raman spectra were measured using the French LabRAM Aramis microconfocal Raman spectrometer (Horiba Jobin Yvon, laser with a wavelength of 532 nm). Elemental analysis (EA) was carried out using a Vario EL III (Elementar, Germany). The adiabatic temperature (T_{ad}) and gas product (mol) of this self-sustained combustion process were estimated using "Thermo" software.

2.3. Electrochemical measurements

The working electrode was prepared by slurring active material (NiO/N@C composites), conductive carbon black and polyvinylidene fluoride (PVDF) binder with the weight ratio of 80:10:10 in 1-methyl-2-pyrrolidinone (NMP). The resultant slurries were coated on a copper foil, and then vacuum dried at 80 °C overnight. CR-2032 type coin cells were assembled using lithium metal as the reference and counter electrodes, Celgard 2500 polypropylene as the separators, and 1 M $LiPF_6$ dissolved into the mixed solvent of ethylene carbonate (EC) and diethyl carbonate (DEC) (v: v, 1:1) as electrolyte. Cycling was performed with an Arbin cycler from 0.005–3 V (vs. Li^+/Li) at various current density. Cyclic voltammetry was performed at a scan rate of 0.1 mV s^{-1} between 0.01 and 3 V with a Gamry-600 potentiostat. For SIB anode testing, 1 M $NaPF_6$ dissolved in propylene carbonate (PC) was utilized as electrolyte, glass fiber (Whatman 934-AH) as separator, and sodium metal as counter electrode, respectively.

3. Results and discussion

3.1. Physicochemical properties of NiO/Ni@C composites

The crystal structure of NiO/Ni@C composites with different nickel nitrate ratios was analyzed by XRD (Fig. 1a). The peaks located at 2θ = 37.2° and 43.30° were assigned to (111) and (200) diffraction peaks of NiO. Meanwhile, NiO/Ni@C-0.25 and NiO/Ni@C-0.375 samples exhibited peaks correlated to metal Ni peaks located at 2θ = 44.3° and 52.3°, corresponding to (111) and (200) crystal planes of Ni, respectively, due to the increase of nickel nitrate precursor. The peaks located approximately at 26° and 44° corresponded to the (002) and (101) diffraction peaks of graphite. With the increase of nickel nitrate content, the diffraction peak intensity of graphite increased, and the degree of graphitization improved. According to the diffraction peak position of (002), the interlayer spacing of the graphene layers in carbon was calculated as 3.39 Å, based on the Scherrer equation, which is slightly higher than that of graphite (3.35 Å) [21]. There were no additional detectable XRD peaks, indicating that Mg and MgO impurities were likely fully removed by acid etching.

The chemical structure of NiO/Ni@C composite was further studied by Raman spectroscopy. Fig. 1b presents three typical bands of carbon materials, including D band (1349 cm^{-1}), G band (1589 cm^{-1}) and 2D band (2686 cm^{-1}), respectively [22]. The D band is generated by the vibration of disorder in the hexagonal graphite substrate plane. Therefore, the strong D peak observed in NiO/Ni@C and the high I_D/I_G proportion of 1.74 (NiO/Ni@C-0.25) indicated that a

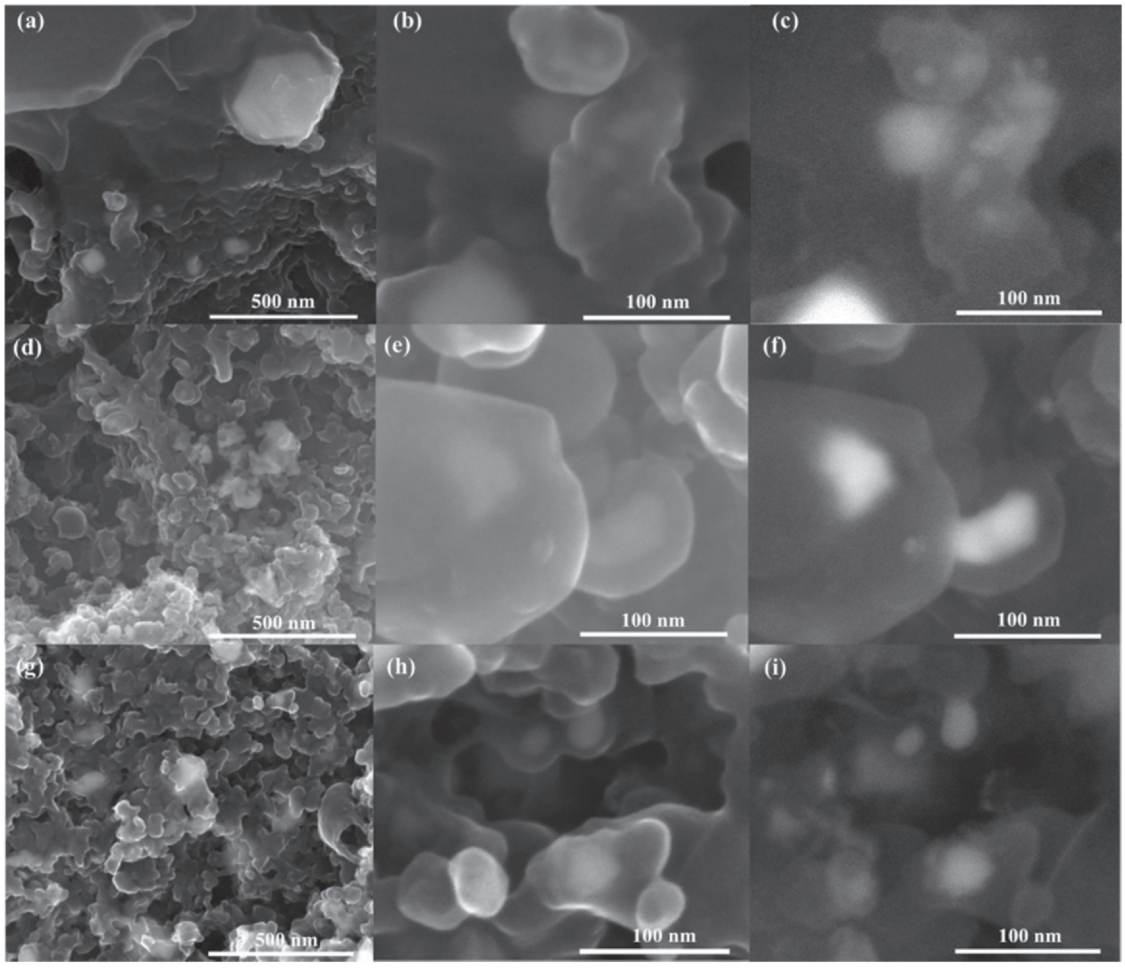

Fig. 2. SEM images of (a,b) NiO/Ni@C-0.125, (d,e) NiO/Ni@C-0.25 and (g,h) NiO/Ni@C-0.375 composites and corresponding backscattering images of (c, f, i).

large number of topological defects were generated due to the combustion synthesis process [23]. The analysis of surface area and pore size distribution were shown in Fig. 1c and d derived from low-temperature nitrogen adsorption-desorption curve. The synthesized NiO/Ni@C composites exhibited typical adsorption and desorption loops and belong to type IV of the IUPAC classification, indicating the presence of meso- and macroporous structure [24]. NiO/Ni@C-0.25 sample exhibits a specific surface area of 245 $m^2 g^{-1}$ and a total pore volume of 0.769 $cm^3 g^{-1}$. The appropriate specific surface area could be attributed to the features of the solution combustion process, releasing a large amount of gases in a short time period, thus resulting in the formation of NiO/Ni@C porous structure. Hierarchical pore structure was observed at 1–25 nm in the pore distribution, in which the mesopores were concentrated at 3.41, 4.67, 8.20, and 10.85 nm. The wide distribution of pores was beneficial to the insertion and rapid diffusion of lithium/sodium ions in electrochemical reactions.

Fig. 2 shows typical SEM images of the NiO/Ni@C nanomaterials, revealing the presence of evenly dispersed NiO/Ni nanoparticles on a carbon substrate. The high-magnification SEM images demonstrate that the NiO/Ni nanoparticles were coated by thin carbon sheets with an average size of ~30 nm, with the backscattering images clearly showing the carbon-coated NiO/Ni composite structure. During the combustion process, NiO/Ni nanoparticles were encapsulated by the *in-situ* synthesized carbon, helping to inhibit the agglomeration of NiO/Ni. This structure also alleviated the volume effect of NiO/Ni nanoparticles effectively and promoted rapid electron transfer between NiO/Ni and the external carbon. Increasing the amount of nickel nitrate caused the content of NiO/Ni nanoparticles to rise, which was consistent with the results of XRD analysis. At the same time, the carbon matrix changed from a continuous structure to more discrete units, likely from the increase gas release during combustion due to the additional nickel nitrate. The coating structure was analyzed further from TEM imaging. As shown in Fig. 3a and b, the NiO/Ni nanoparticles are encapsulated by the highly porous carbon matrix. High-resolution TEM (HRTEM) image showed that the NiO/Ni nanomaterials were covered by a thin carbon layer of 2–5 nm (Figs. 3c, d and S1). Meanwhile, the lattice fringes in Fig. 3c showed an interplanar spacing of 0.21 nm, which arises from the (200) crystal faces of NiO, and the 0.205 nm interplanar spacing shown in Fig. 3d correspond to the (111) faces of Ni. The well-dispersed NiO/Ni nanocrystals showed an average size of ~30 nm, which is in accordance with the observations from SEM imaging.

The carbon content of NiO/Ni@C composite was measured using TGA and EA methods. As shown in Fig. 4, as the temperature increased from 300 °C to 700 °C, the weight of the NiO/Ni@C samples decreased steadily due to the oxidation of carbon. Subsequently, the masses of corresponding samples stayed constant as the temperature continued to rise. Note that the carbon content of NiO/Ni@C samples was approximately equal to the mass loss. The carbon content of each product was calculated as 90% for NiO/Ni@C-0.125, 70% for NiO/Ni@C-0.25%, and 50% for NiO/Ni@C-0.375, respectively, which is consistent with EA measurements (Table S1). Therefore, this synthetic strategy enables control of the relative content of NiO, Ni and carbon through adjusting the proportion of nickel nitrate precursors.

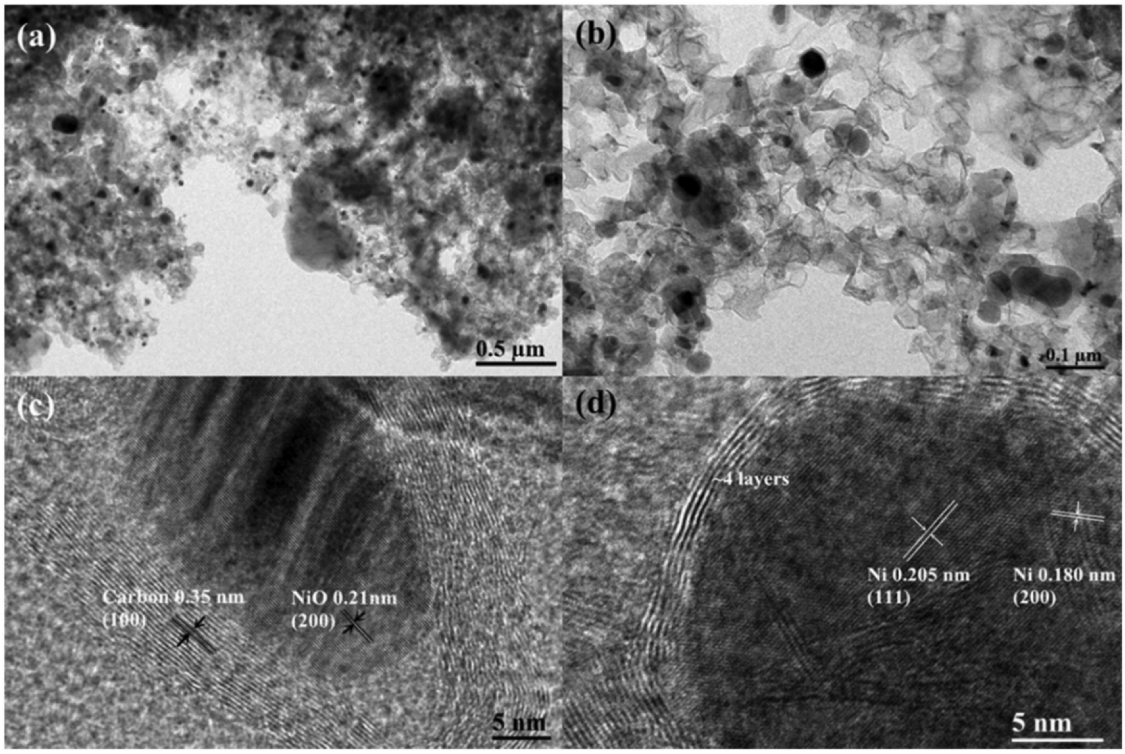

Fig. 3. (a,b,c) TEM and (d) HRTEM images of NiO/Ni@C-0.25 composite.

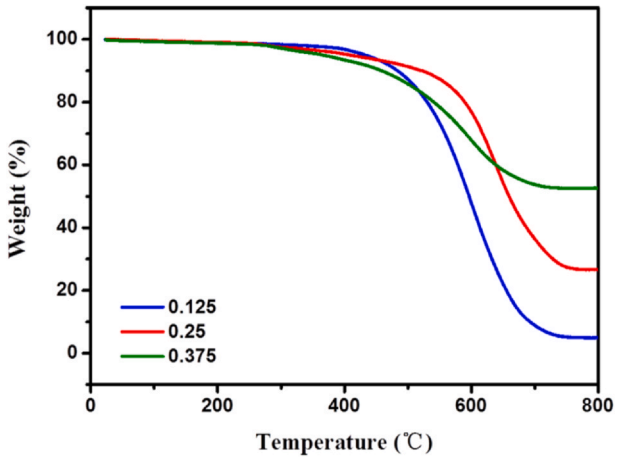

Fig. 4. Thermogravimetric curves of NiO/Ni@C composites under air atmosphere.

The calculation and measurement of the combustion temperature were helpful to understand and control the experimental process and the resulting properties of the synthesized products. As shown in Fig. S2 and Table S2, during self-propagating combustion, the calculated adiabatic temperatures (T_{ad}) of NiO/Ni@C-0.125, NiO/Ni@C-0.25 and NiO/Ni@C-0.375 samples were 2301.38 K, 2247.17 K, and 2194.02 K, respectively. Furthermore, a large amount of gas (primarily water vapor) was released during combustion, dissipating the heat of the system and contributing to the formation of the porous structure. The highest measured combustion temperature of NiO/Ni@C-0.25 sample was 1100 °C, lower than the calculated T_{ad}, likely because the actual process was not adiabatic and the thermocouple signal might lag or reach the upper limit. Nevertheless, the measured temperature variation trend was consistent with the calculated results, with increased nickel nitrate content decreasing the intensity of the combustion event, i.e. longer combustion time.

3.2. Electrochemical analysis of NiO/Ni@C composites

The various synthesized NiO/Ni@C composites were subsequently investigated as anode material for LIBs and SIBs. Fig. 5a shows that NiO/Ni@C-0.25 composites exhibit a satisfactory rate capability and cycling stability as LIB anode. The reversible capacities of 418, 374, 329, 250 and 210 mAh g^{-1} were obtained at 0.05, 0.1, 0.2, 0.5 and 1 A g^{-1}, respectively, which is comparable to best values of previously reported NiO/C and NiO/Ni/C materials displayed in Table S3. In addition, the capacity recovered and increased to 463 mAh g^{-1} after returning to 0.1 g^{-1}, indicating that the NiO/Ni@C composite electrode had high cycling stability and good reversibility. The capacity increase may be attributed to the formation and dissolution of polymeric species in the solid electrolyte interphase (SEI) layer induced by the catalytic activity of formed metal in full discharged state, which is consistent with previous reports about NiO and other metal oxide anodes [25]. In addition, the reversible capacity of NiO/Ni@C-0.25 increased to 791 mAh g^{-1} after 150 cycles, approaching the theoretical capacity of NiO, with a Coulombic efficiency near 100%. This was likely due to the carbon-coated structure that offered a buffer effect for volumetric changes induced by Li^+ insertion/extraction, thus providing good structural integrity and cycling stability. Additionally, the porous carbon could be activated after the initial charge-discharge process resulting in increased capacity.

As SIB anode, NiO/Ni@C-0.25 composites exhibited reversible capacities of 218, 158, 125, 98 and 73 mAh g^{-1} at specific currents of 0.02, 0.05, 0.1, 0.2 and 0.5 A g^{-1}, respectively. The capacity remained at 114 mAh g^{-1} after returning a specific current of 0.1 A g^{-1}, suggesting the good stability of the NiO/Ni@C nanomaterial. After 150 cycles, the reversible capacity was maintained at 83 mAh g^{-1} with a corresponding Coulombic efficiency of about 100%. These results

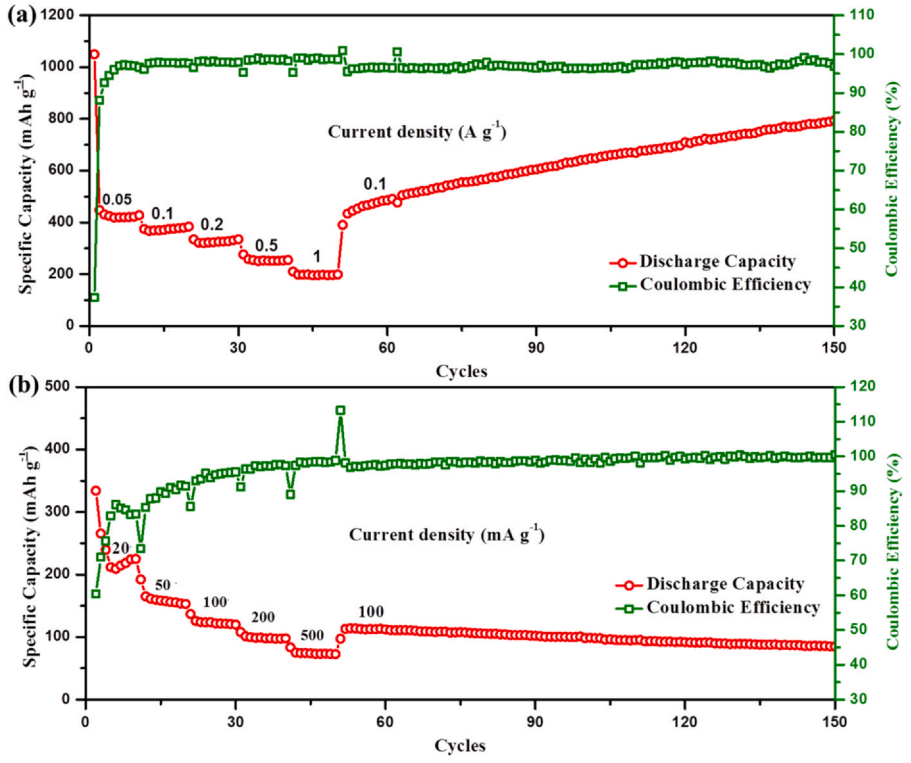

Fig. 5. Rate capacity and cycling stability of NiO/Ni@C composites at different specific currents in (a) LIBs and (b) SIBs.

indicate that the carbon coating structure in the as prepared NiO/Ni@C composites could help reduce the ionic diffusional distance, effectively relieve the structural stress, and thus enhance the electrode stability greatly [26]. The carbon-coated NiO/Ni composites synthesized by solution combustion was confirmed to be a potential anode material for high-performance LIBs and SIBs.

Figs. 6a and S3 show the discharge and charge behavior of NiO/Ni@C composites in the first three cycles with a specific current of 0.05 A g^{-1} and a voltage range between 0.01 and 3.0 V. The reversible capacity was 460 mAh g^{-1}, while the initial discharge capacity of the sample was 1051 mAh g^{-1}, corresponding to the first cycle Coulombic efficiency of 43%. After the first cycle, the capacity stabilized with reversible cycling behavior observed. This capacity loss was attributed to the formation of SEI layer, which irreversibly traps lithium ions and decomposes electrolyte on the anode surface [27,28]. Cyclic voltammetry (CV) was performed to further study the lithium ion storage process. As shown in Fig. 6b, during the first cathodic scan of the NiO/Ni@C-0.25 electrode, a sharp reduction peak appears near 0.25 V, corresponding to the transformation of NiO into Ni, Li into Li_2O and SEI film formation. A strong oxidation peak appeared at 2.2 V, corresponding to the conversion of Li_2O to Li, and oxidation of Ni to NiO [29]. After the first cycle, the reduction and oxidation peaks shifted to 1.2 V and 2.3 V respectively, due to microstructural changes of the material during the first discharge [30]. Subsequent cycles of the CV curves overlapped, indicating that the NiO/Ni@C composites quickly stabilize and exhibit good reversibility.

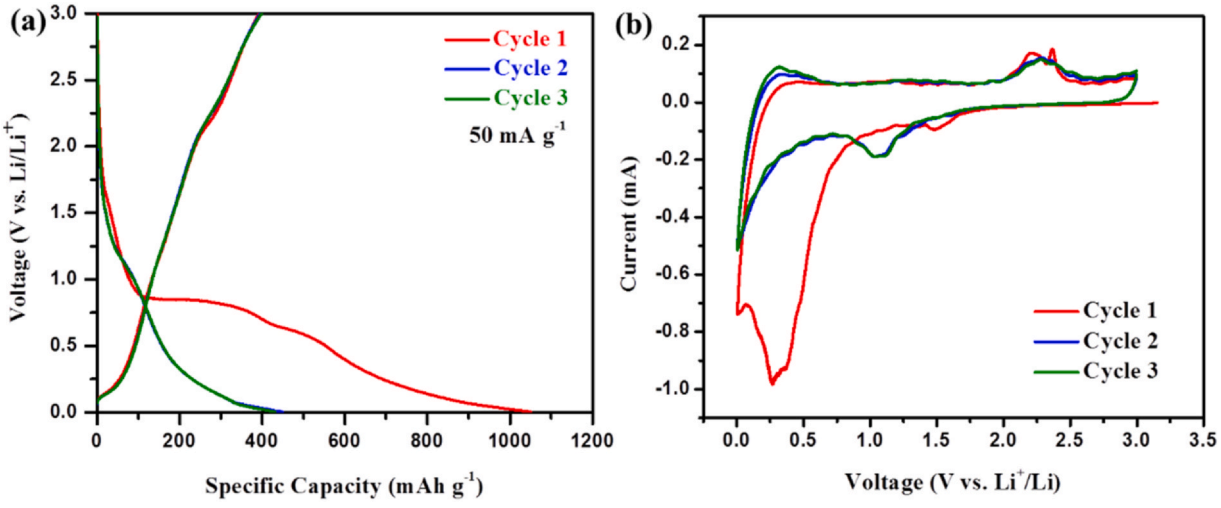

Fig. 6. (a) Current discharge/charge voltage diagram of NiO/Ni@C-0.25 composite for the initial three cycles between 0.01 and 3 V, and (b) CV curve of NiO/Ni@C-0.25 composite in the initial three cycles.

Fig. S4 shows the discharge/charge voltage profiles and rate capability curves of NiO/Ni@C composites with different carbon content. Fig. S4a and c correspond to NiO/Ni@C-0.125 and NiO/Ni@C-0.375 electrodes. These materials exhibited a similar large first cycle capacity loss due to irreversible reactions, such as irreversible SEI film formation on the high surface area material. Similar values were generally found in other transition metal oxide electrodes (Fe_3O_4, MnO_2 and CuO, etc.) [31–34]. Similar to NiO/Ni@C-0.25 composites, NiO/Ni@C-0.125 and NiO/Ni@C-0.375 electrode materials exhibited excellent rate capability and electrochemical cycle stability in Fig. S4b and d. This performance was primarily attributed to the following reasons: (1) the porous structure and high specific surface area of the carbon matrix buffers the volumetric changes during charging and discharging while providing a conductive framework. (2) The nanoparticle dimensions shorten the ion diffusional pathway, further buffering the volume change and the structural stress. (3) The *in-situ* synthesized Ni reduces the absolute value of the volume change in the charging and discharging reaction of NiO, helping to augment cycling stability and LIB performance.

4. Conclusions

Using carbon dioxide and nickel nitrate as the carbon source and nickel source respectively, carbon-coated NiO/Ni nanomaterials were successfully prepared by a one-step combustion process. In addition, the phase and relative content of the products could be easily controlled and assembled by simply adjusting the operating conditions of the solution combustion synthesis process. As anode material for LIBs and SIBs, these materials exhibited high reversible capacity, excellent cycling stability, and outstanding rate capability. NiO/Ni@C-0.25 exhibited a reversible lithium/sodium storage capacity of 791 and 83 mAh g^{-1} after 150 cycles at 0.1 A g^{-1}, respectively. The excellent reversibility of NiO/Ni@C composites could be attributed to the synergistic effects of its porous structure, carbon coating, and two-component NiO/Ni structure. The NiO/Ni@C composites reported in this work are potential anode materials for high-performance LIBS and SIBs.

CRediT authorship contribution statement

Chunxiao Xu conceived the idea and designed the present work. **Chunxiao Xu**, **Yayong Li**, and **Ryan A. Adams** synthesized the materials and performed the performance tests. **Vilas G. Pol**, **Yang Xiao**, **Arvind Varma**, and **Pengwan Chen** supervised the research.

Declaration of Competing Interest

The authors declare that they have no known competing financial interests or personal relationships that could have appeared to influence the work reported in this paper.

Acknowledgements

This work was supported by the R. Games Slayter Fund and the William-Cynthia Smith Gift Funds, the A. Varma Reaction Engineering Research Fund, and the State Key Laboratory of Explosion Science and Technology, Beijing Institute of Technology under Grant No. ZDKT18-01.

Appendix A. Supporting information

Supplementary data associated with this article can be found in the online version at doi:10.1016/j.jallcom.2021.160927.

References

[1] V. Etacheri, R. Marom, R. Elazari, G. Salitra, D. Aurbach, Challenges in the development of advanced Li-ion batteries: a review, Energy Environ. Sci. 4 (2011) 3243–3262.
[2] F.X. Ma, H. Hu, H.B. Wu, C.Y. Xu, Z. Xu, L. Zhen, X.W. David Lou, Formation of uniform Fe_3O_4 hollow spheres organized by ultrathin nanosheets and their excellent lithium storage properties, Adv. Mater. 27 (2015) 4097–4101.
[3] Y. Zou, Y. Wang, NiO nanosheets grown on graphene nanosheets as superior anode materials for Li-ion batteries, Nanoscale 3 (2011) 2615–2620.
[4] R.A. Adams, V.G. Pol, A. Varma, Tailored solution combustion synthesis of high performance $ZnCo_2O_4$ anode materials for lithium-ion batteries, Ind. Eng. Chem. Res. 56 (2017) 7173–7183.
[5] A.S. Prakash, P. Manikandan, K. Ramesha, Solution-combustion synthesized nanocrystalline $Li_4Ti_5O_{12}$ as high-rate performance Li-ion battery anode. Chem. Mater. 22 (2010) 2857–2863.
[6] C.X. Xu, K.V. Manukyan, R.A. Adams, V.G. Pol, P.W. Chen, A. Varma, One-step solution combustion synthesis of CuO/Cu_2O/C anode for long cycle life Li-ion batteries. Carbon 142 (2019) 51–59.
[7] M.V. Reddy, G.V. Subba Rao, B.V. Chowdari, Metal oxides and oxysalts as anode materials for Li ion batteries, Chem. Rev. 113 (2013) 5364–5457.
[8] W. Wen, J.-M. Wu, M.-H. Cao, NiO/Ni powders with effective architectures as anode materials in Li-ion batteries, J. Mater. Chem. A 1 (2013) 3881–3885.
[9] P. Roy, S.K. Srivastava, Nanostructured anode materials for lithium ion batteries, J. Mater. Chem. A 3 (2015) 2454–2484.
[10] L. Liu, Y. Guo, Y. Wang, X. Yang, S. Wang, H. Guo, Hollow NiO nanotubes synthesized by bio-templates as the high performance anode materials of lithium-ion batteries, Electrochim. Acta 114 (2013) 42–47.
[11] G. Evmenenko, T.T. Fister, D.B. Buchholz, Q. Li, K.S. Chen, J. Wu, V.P. Dravid, M.C. Hersam, P. Fenter, M.J. Bedzyk, Morphological evolution of multilayer Ni/NiO Thin film electrodes during lithiation, ACS Appl. Mater. Interfaces 8 (2016) 19979–19986.
[12] J. Wu, W.J. Yin, W.W. Liu, P. Guo, G. Liu, X. Liu, D.S. Geng, W.-M. Lau, H. Liu, L.M. Liu, High performance NiO nanosheets anchored on three-dimensional nitrogen-doped carbon nanotubes as a binder-free anode for lithium ion batteries, J. Mater. Chem. A 4 (2016) 10940–10947.
[13] D.H. Lee, J.C. Kim, H.W. Shim, D.W. Kim, Highly reversible Li storage in hybrid NiO/Ni/graphene nanocomposites prepared by an electrical wire explosion process, ACS Appl. Mater. Interfaces 6 (2014) 137–142.
[14] M.-Y. Cheng, B.-J. Hwang, Mesoporous carbon-encapsulated NiO nanocomposite negative electrode materials for high-rate Li-ion battery, J. Power Sources 195 (2010) 4977–4983.
[15] B. Zhao, J. Song, P. Liu, W. Xu, T. Fang, Z. Jiao, H.J. Zhang, Y. Jiang, Monolayer graphene/NiO nanosheets with two-dimension structure for supercapacitors, J. Mater. Chem. 21 (2011) 18792–18798.
[16] F. Zou, Y.-M. Chen, K.W. Liu, Z.T. Yu, W.F. Liang, S.M. Bhaway, M. Gao, Y. Zhu, Metal organic frameworks derived hierarchical hollow NiO/Ni/Graphene composites for lithium and sodium storage. ACS Nano 10 (2016) 377–386.
[17] C.X. Xu, S. Chen, L.Y. Du, C.X. Li, X. Gao, J.J. Liu, L.T. Qu, P.W. Chen, Scalable conversion of CO_2 to N-Doped carbon foam for efficient oxygen reduction reaction and lithium storage, ACS Sustain. Chem. Eng. 6 (2018) 3358–3366.
[18] W. Sun, X. Rui, J. Zhu, L. Yu, Y. Zhang, Z. Xu, S. Madhavi, Q. Yan, Ultrathin nickel oxide nanosheets for enhanced sodium storage and lithium storage, J. Power Sources 274 (2015) 755–761.
[19] Y. Jiang, M. Hu, D. Zhang, T. Yuan, W. Sun, B. Xu, M. Yan, Transition metal oxides for high performance sodium ion battery anodes, Nano Energy 5 (2014) 60–66.
[20] A. Varma, A.S. Mukasyan, A.S. Rogachev, K.V. Manukyan, Solution combustion synthesis of nanoscale materials, Chem. Rev. 116 (2016) 14493–14586.
[21] L. Qu, Y. Liu, J.B. Baek, L. Dai, Nitrogen-doped graphene as efficient metal-free electrocatalyst for oxygen reduction in fuel cells, ACS Nano 4 (2010) 1321–1326.
[22] P.W. Chen, C.X. Xu, H. Yin, X. Gao, L.T. Qu, Shock induced conversion of carbon dioxide to few layer graphene, Carbon 115 (2017) 471–476.
[23] R.A. Adams, J.M. Syu, Y. Zhao, C.T. Lo, A. Varma, V.G. Pol, Binder-free N- and O-rich carbon nanofiber anodes for long cycle life K-ion batteries, ACS Appl. Mater. Interfaces 9 (2017) 17872–17881.
[24] C.X. Xu, P.W. Chen, K.Y. Liu, X. Gao, L.Y. Du, CO_2 Conversion into N-doped carbon nanomesh sheets, ACS Appl. Nano Mater. 2 (2019) 2991–2998.
[25] X.L. Sun, C.L. Yan, Y. Chen, W.P. Si, J.W. Deng, S. Oswald, L.F. Liu, O.G. Schmidt, Three-dimensionally "curved" NiO nanomembranesas ultrahigh rate capability anodes for Li-ion batteries with long cycle lifetimes, Adv. Energy Mater. 4 (2014) 1300912.
[26] L.Y. Du, C.X. Xu, J.J. Liu, Y.Z. Lan, P.W. Chen, One-step detonation-assisted synthesis of Fe_3O_4-Fe@BCNT composite towards high performance lithium-ion batteries. Nanoscale 9 (2017) 14376–14384.

[27] H. Song, N. Li, H. Cui, C. Wang, Enhanced storage capability and kinetic processes by pores- and hetero-atoms- riched carbon nanobubbles for lithium-ion and sodium-ion batteries anodes, Nano Energy 4 (2014) 81–87.
[28] Z.-L. Wang, D. Xu, H.-G. Wang, Z. Wu, X.-B. Zhang, In situ fabrication of porous graphene electrodes for high-performance energy storage, ACS Nano 7 (2013) 2422–2430.
[29] S. Ni, X. Lv, J. Ma, X. Yang, L. Zhang, A novel electrochemical reconstruction in nickel oxide nanowalls on Ni foam and the fine electrochemical performance as anode for lithium ion batteries, J. Power Sources 270 (2014) 564–568.
[30] W. Wen, J.-M. Wu, Eruption combustion synthesis of NiO/Ni nanocomposites with enhanced properties for dye-absorption and lithium storage, ACS Appl. Mater. Interfaces 3 (2011) 4112–4119.
[31] S. Chen, Y. Shi, Y. Wang, Y. Shang, W. Xia, H.Y. Yang, An all manganese-based oxide nanocrystal cathode and anode for high performance lithium-ion full cells, Nanoscale Adv. 1 (2019) 1714–1720.
[32] W. Yang, J. Wang, W. Ma, C. Dong, G. Cheng, Z. Zhang, Free-standing CuO nanoflake arrays coated Cu foam for advanced lithium ion battery anodes, J. Power Sources 333 (2016) 88–98.
[33] M. Zhang, B. Qu, D. Lei, Y. Chen, X. Yu, L. Chen, Q. Li, Y. Wang, T. Wang, A green and fast strategy for the scalable synthesis of Fe_2O_3/graphene with significantly enhanced Li-ion storage properties, J. Mater. Chem. 22 (2012) 3868–3874.
[34] L. Pan, K.X. Wang, X.D. Zhu, X.M. Xie, Y.T. Liu, Hierarchical assembly of SnO_2 nanowires on MnO_2 nanosheets: a novel 1/2D hybrid architecture for high-capacity, reversible lithium storage, J. Mater. Chem. A 3 (2015) 6477–6483.